J Med Syst (2010) 34:195–212
DOI 10.1007/s10916-008-9231-z

ORIGINAL PAPER

EEG Signal Analysis: A Survey

D. Puthankattil Subha · Paul K. Joseph · Rajendra Acharya U · Choo Min Lim

Received: 25 August 2008 / Accepted: 29 October 2008 / Published online: 6 December 2008

Abstract The EEG (Electroencephalogram) signal indicates the electrical activity of the brain. They are highly random in nature and may contain useful information about the brain state. However, it is very difficult to get useful information from these signals directly in the time domain just by observing them. They are basically non-linear and nonstationary in nature. Hence, important features can be extracted for the diagnosis of different diseases using advanced signal processing techniques. In this paper the effect of different events on the EEG signal, and different signal processing methods used to extract the hidden information from the signal are discussed in detail. Linear, Frequency domain, time - frequency and non-linear techniques like correlation dimension (CD), largest Lyapunov exponent (LLE), Hurst exponent (H), different entropies, fractal dimension(FD), Higher Order Spectra (HOS), phase space plots and recurrence plots are discussed in detail using a typical normal EEG signal.

Keywords EEG · Correlation dimension · Fractal dimension · Entropy · Recurrence plot

Introduction

The electrical activity of a brain (EEG) exhibits significant complex behavior with strong non-linear and dynamic properties. The communication in the brain cells take place through electrical impulses. It is measured by placing the electrodes on the scalp of the subject. The cortical nerve cell inhibitory and excitatory postsynaptic potentials generate the EEG signals. These postsynaptic potentials summate in the cortex and extend to the scalp surface where they are recorded as EEG. A typical EEG signal, measured from the scalp, will have an amplitude of about 10 μV to 100 μV and a frequency in the range of 1 Hz to about 100 Hz.

Electrode locations are specified by the 10–20 electrode placement system devised by International Federation of Societies for Electroencephalography. The 10–20 system is based on the relationship between the location of an electrode and the underlying area of cerebral cortex. During the recording of the signal, different types of interference waves or artifacts get added to the EEG signal. Various types of artifacts affecting the EEG signal are discussed in the following section.

EEG signals are highly non-Gaussian, nonstationary and have a non-linear nature. Electroencephalography is a noninvasive technique used to diagnose brain related diseases and symptoms. It helps in diagnosing many neurological diseases, such as epilepsy, tumor, cerebrovascular lesions, depression and problems associated with trauma. EEG traces are different for different brain activities. The brain activity of an abnormal person can easily be distinguished from a normal person using signal processing methods.

The EEG signals are recorded from electrodes placed on the scalp. There are two types of EEG recordings: (i) monopolar (ii) bipolar. Monopolar recording picks up the voltage difference between an active electrode on the scalp and a reference electrode on the ear lobe. Bipolar electrodes give the voltage difference between two scalp electrodes. EEG signals are characterized by the following rhythms: delta waves, theta waves, alpha waves and beta waves. The

D. P. Subha · P. K. Joseph
Department of Electrical Engineering,
National Institute of Technology,
Calicut, India

R. Acharya U (✉) · C. M. Lim
Department of Electronics and Computer engineering,
Ngee Ann Polytechnic,
Singapore, Singapore
e-mail: aru@np.edu.sg

frequency range of delta activity is 3 Hz or below and found predominantly in infants up to 1 year and deep sleep stages of normal adults. Theta activity has a frequency range of 4 Hz to 8 Hz. It exists in normal infants and children as well as during drowsiness and sleep in adults. Presence of high theta activity in awake adults suggests abnormal and pathological conditions. Alpha waves have a frequency range of 8 Hz to 13 Hz. It is usually seen in the posterior regions of the head on each side, being higher in amplitude on the dominant side. The amplitude is mostly less than 50 μV and is found in occipitals. This is a major rhythm seen in normal relaxed adults. Beta rhythms have a frequency range of 13 Hz to 30 Hz and predominant in the frontal portion. This rhythm is present in alert or anxious subjects.

The brain signals are highly complex and random in nature. Their characteristics strongly depend on the individual, age and mental state. The occurrence of symptoms is also at random in time scale. Hence, understanding the behavior and dynamics of billions of interconnected neurons involves several linear and nonlinear signal processing techniques and its correlation to the physiological events. The importance of the biological time series analysis, which exhibits typically complex dynamics, has long been recognized in the area of non-linear analysis. Several features of these approaches have been proposed to detect the hidden important dynamical properties of the physiological phenomenon. The nonlinear dynamical techniques are based on the concept of chaos has been applied to many areas including the areas of medicine and biology. "Effect of various events on EEG signal" of the paper deals with the effect of various events on EEG signal. Different EEG signal analysis methods are discussed in "EEG signal and sleep" and "EEG signal and epilepsy" deals with discussion. And finally the paper concludes in "EEG signal and drugs/anesthesia".

Effect of various events on EEG signal

There are various events, namely: sleep, epilepsy, reflexology, drugs/anesthesia, diabetes, meditation, music and artifacts, influence the EEG signal. Their influence on the EEG signal are given below.

EEG signal and sleep

Different stages of sleep can be analyzed by extracting relevant EEG features. These parameters help in diagnosing sleep disorders. Robert *et al* have used wavelet transforms (WT) and neural network techniques on EEG signal to identify the sleep apnea syndrome (SAS) [51]. The EEG signals were separated into delta, theta, alpha, and beta spectral components by using multi-resolution wavelet transforms before feeding to a classifier. Recently, the polysomnography of a healthy male subject was analyzed by evaluating the correlation dimension [47]. The correlation dimension decreased from 'awake' stage to sleep stages 1–3 (stage 1: 6 Hz–8 Hz, stage 2: 4 Hz–7 Hz, stage 3: 1 Hz–3 Hz) and increased during the rapid eye movement (REM) sleep stage. In each sleep cycle, the correlation dimension decreased for slow sleep wave, and increased for REM sleep. Acharya *et al* have analyzed the cortical functions at different sleep stages using the CD, FD, LLE, approximate entropy (ApEn), H, phase space plot and recurrence plots [2]. They proposed different phase space and recurrence plots for different sleep stages.

Recurrence quantification analysis (RQA) was used to identify the sleep apnea syndrome using EEG signals [77]. All the sleep stages were distinctly discriminated by means of the RQA accurately. The fractal-scaling exponent was computed using detrended fluctuation analysis, to compare normal sleep stages with sleep apnea [49]. The scaling exponent for the apnea was reported to be lower than those of the healthy subject during all stages of sleep. Wavelet transform and artificial neural networks were used for identifying SAS [72]. Multi-resolution wavelet transforms were used for separating the EEG signals into delta, theta, alpha and beta spectral components. These spectral components were then applied as inputs of the artificial neural network, to identify SAS episodes.

EEG signal and epilepsy

Epilepsy is a brain disorder where the normal neuronal activity gets affected. It can easily be diagnosed with EEG and brain scan. The typical stages of an epileptic seizure are interictal, preictal and ictal. The Lyapunov exponent of EEG signal was used for the identification of epileptic seizures [84]. LLE showed distinct difference in the normal and epileptic EEG signals. The discrete wavelet transform (DWT) coefficients of EEG signals were fed into a modular neural network structure (mixture of experts' network) for detecting epileptic EEG signals [83]. This classifier performed better compared with stand alone neural network models. Correlation dimension and mean phase coherence were used to characterize the interictal EEG for prediction of seizures [6]. The CD values of interictal recordings were found to be lower for epileptic focus compared to other areas of the brain. Kemal *et al*, have compared the performance of Short Time Fourier Transform (STFT) and Continuous Wavelet Transform (CWT) using Labview program to analyze the epileptic seizure [46]. Their results show that, CWT is effective for clinical interpretation due to its high resolution and the STFT can be used for real time diagnosis. Different entropies have been used to analyze normal and epileptic EEG signals [41]. They were able to

classify normal and epileptic EEG signals using different entropies and neuro-fuzzy technique with an efficiency of more than 90%.

EEG signal and reflexology

Reflexology, is a natural healing art, based on the principle that there are reflexes in the feet and hands which directly correspond to every part of the body. Kannathal *et al* have analyzed the effect of the reflexology on EEG signals using non-linear features and modeling techniques [40, 39]. They have shown that, non-linear parameters decreased due to reflexological stimulation indicating a reduction in the variability in the EEG signal. This indicates that, the ∝ wave tend to become more predominant due to the influence of the reflexology. They have concluded that AR modeling techniques are superior compared with FFT method in analyzing the effects of reflexological stimulation at the feet using the EEG signal as base signal. Peak amplitude, peak frequency and their ratios were used to study the effect of reflexology on the EEG signals using modeling method [40].

EEG signal and drugs/anesthesia

The effect of thiopental (intravenous anesthetics) on the brain performance was studied using EEG signals [80]. It was found that EEG activation occurred at low thiopental concentrations. The low thiopental concentrations showed reduced number of waves/second, while it increased at high thiopental concentrations. A novel method to interpret the effect of anesthetic agents (sevoflurane) on the neural activity, by using recurrence quantification analysis of EEG data, was proposed [50]. It was found that the determinism of the recurrence plot increased gradually with increases in the concentration of sevoflurane.

EEG signal and diseases

Recently, Ktonas *et al* have estimated the instantaneous envelope and frequency waveforms of sleep spindles from patients with dementia and normal subjects using the time-frequency technique of complex demodulation [48]. They have reported the differences in sleep spindle instantaneous frequency dynamics in dementia and normal subjects. A significant proportion of patients with dementia showed a lower bispectral index than normal "awake" subjects [69]. Patients with Alzheimer's disease or vascular dementia showed an increase in slow wave and a decrease in fast wave activity of the EEG. A method to estimate the degree of cognitive impairment, caused by the Alzheimer's disease from the EEG quantitative indicators was proposed [57]. They have shown that, a decrease in alpha coherence and an increase in delta coherence were most significantly correlated to the degree of dementia. Neural network and hybrid systems were used to differentiate Alzheimer's patients (AD), minimal cognitive impairment (MCI), and normal controls using EEG signal analysis [33]. They have shown that, the patients were categorized accurately using the combination of EEG synchronization results and selected clinical parameters. Haar wavelets were used on EEG signals for the accurate detection of Alzheimer's disease and de-noise the presence of ocular artifacts [88]. The remarkable performance of this technique over conventional methods while recording Alzheimer's EEG signals were discussed.

The EEG background activity in patients with Autism disease was in frequency domain by calculating bispectrum transform, short time Fourier transform (STFT) and also STFT at bandwidth of total spectrum (STFT-BW) [76]. Their findings suggested that STFT-BW can discriminate with an accuracy of 82.4% between normal and Autism subject.

EEG signal and meditation

Joseph *et al* have analyzed the dynamics of the EEG signal at different stages of meditation using nonlinear parameters like CD, LLE and H [37]. They have reported that, the variability of EEG signals decreases significantly during the khumbaka stage. It has been observed that the practice of transcedental meditation (TM) produced an increase in alpha phase synchrony, primarily between anterior and posterior regions [30]. They have observed that enhanced phase synchrony in the alpha frequency during meditation improves the functional integration. The meditation EEG signals were analyzed using the wavelet analysis and fuzzy c-means [38]. They have proposed a distinct gray-scale chart from the extracted features to reveal different meditation states. Parallel functional activity of the brain reduced during bramari (part of pranayam-breathing for relaxation) [62]. The nonlinear measures like CD, LLE, ApEn and z-score value decreased during this period.

EEG signal and music

It was found that the EEG signals respond differently to different types of music. The nature of EEG and its effect on the brain due to the different types of music was studied [53]. They have shown that, the frequency of EEG signal changes for different types of music. The middle abdomen area in the pon's side of the brain was focused for this study. Bhattacharya *et al* have presented a phase synchrony analysis of EEG in five standard frequency bands: delta (<4 Hz), theta (4–8 Hz), alpha (8–13 Hz), beta (13–30 Hz), and gamma (>30 Hz) [7]. The analysis was done using indices like coherence and correlation in two groups of

musicians and non musicians. They observed a higher degree of gamma band synchrony in musicians. Frequency distribution analysis and the independent component analysis (ICA) were used to analyze the EEG responses of subjects for different musical stimuli. It was shown that some of these EEG features were unique for different musical signal stimuli [90].

EEG and artifacts

Artifacts are undesirable electrical potentials which come from sources other than the brain. Small amplitude EEG signals are highly sensitive to artifacts. This includes electro galvanic signals (slow artifact), movement artifact and frequency artifacts. Artifacts are to be detected and removed in order to improve the interpretation of EEG signals. An extended Kalman filter approach and a neural network instead of the AR model for the detection of EEG artifacts was proposed [73]. This algorithm was able to detect artifacts correctly with a specificity of 90% and sensitivity of 65%. An efficient parametric system for automatic detection of electroencephalogram (EEG) artifacts in polysomnographic recordings was studied [19]. Relevant features were extracted from selected artifacts in a given epoch and was compared with the threshold to detect the artifacts. Recently, Charles *et al*, have used singular-value decomposition to separate multichannel EEG signals into components by optimizing a signal-to-noise quotient [12]. Subsequently these components were used to filter out artifacts.

EEG signal is electrical potential that results from the neurons of the brain. Figure 1 shows a typical normal EEG signal.

Analysis

Various measurement techniques of analysis time domain, frequency domain, time-frequency and non-linear methods are discussed below.

Time domain

Linear prediction and independent component analysis (ICA) can be used to extract relevant EEG signal features. These methods are briefly explained below.

Linear prediction (LP)

The term 'linear prediction' refers to predicting the output of a linear system based on its input *x(n)* and previous outputs *y(n−1), y(n−2),....,y(n−p)*.

$$\hat{y}(n) = \sum_{k=1}^{p} a(k)y(n-k) + \sum_{k=0}^{N} b(k)x(n-k) \quad (1)$$

where, *a* and *b* are called predictor coefficients.

The notation $\hat{y}(n)$ refers to the estimate or prediction of *y(n)*. The output is equal to a linear combination of past output values along with past and present input values. Once the input *x(n)* and output *y(n)*are known, the behavior of the unknown system *H(z)* can be predicted, provided the transfer function is known.

LP can be used for signal generation, storage and transmission of EEG [66]. It can also be used for the analysis and presentation of spectral array data which provides better visualization of background EEG activity.

Independent component analysis (ICA)

The purpose of ICA is to linearly decompose a multidimensional data vector into statistically independent components. It is assumed that each measured signal is a linear combination of independent signals. Each of these independent signals is referred to by the variable S_i and the linearly combined signals by x_i. Each measured signal can be expressed as a linear combination of the original independent signals as follows:

$$x_i = a_1 s_1 + a_2 s_2 + ... + a_n s_n \quad (2)$$

We can express the entire system of n measured signals as:

$$X = AS$$

where each row of ''*X*' is a set of readings for each signal x_i each row of '*S*' is an original signal S_i and '*A*' is an *nxn* mixing matrix that generates '*X*' from '*S*'.

Independent component analysis (ICA) is an effective method for removing artifacts and separating individual sources of brain signals from EEG recordings [87].

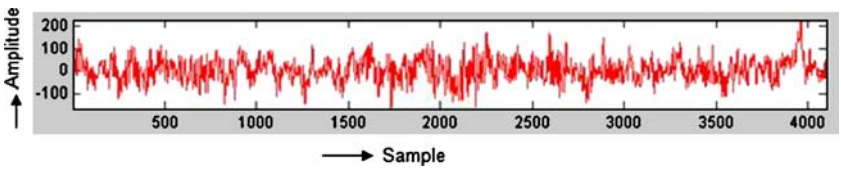

Fig. 1 Typical normal EEG signal

Spectral analysis

The approaches for spectrum estimation may be generally categorized into two classes. (i) The classical or non-parametric method which deals with the estimation of the autocorrelation from a given data set. The power spectrum is then estimated by Fourier transformation of the estimated autocorrelation sequence. (ii) The non-classical or parametric approach is based on using a model for the process in order to estimate the power spectrum.

Non parametric method

The Welch method is popularly used to estimate the power spectrum of a given time sequence [91]. The sequences are allowed to overlap and a data window is applied to each sequence. Let $\{x_d(n)\}$,be the sequence.

Where $d=1, 2, 3,\ldots,L$ are the signal intervals and each interval length is M. So, the Power Spectral Density (PSD), according to Welch is given by:

$$\hat{P}_d(f) = \frac{1}{MU}\left|\sum_{n=0}^{M-1} x_d(n)\, w(n) e^{-j2\pi fn}\right|^2 \tag{3}$$

Where U is the normalization factor for the power in the window function, selected as:

$$U = \frac{1}{M}\sum_{n=0}^{M-1} |w(n)|^2 \tag{4}$$

where $w(n)$ is the windowed data.

The Welch power spectrum is the average over these modified periodograms that is:

$$\hat{P}_{Welch}(f) = \frac{1}{L}\sum_{i=0}^{L-1} \hat{P}_d(f) \tag{5}$$

where $\hat{P}_{Welch}$ is the periodogram of the EEG signal of each interval .

Parametric method

The non parametric methods suffer from spectral leakage effects due to windowing. Spectral leakage masks weak signal components. A parametric (model based) power spectrum estimation method overcomes the problem of spectral leakage and provides better frequency resolution. These methods assume the signal to be a stationary random process. This process can be modeled as the output of a filter with white noise input. The filter parameters are obtained from the signal. There are different ways to obtain these parameters. The methods are classified depending on the presence of poles in the z-domain. If there are no poles, then it is MA (moving average) Model. If there are poles present and all zeros are located at the origin, then it is an AR (auto recursive) model. A model having poles and zeros freely distributed in the z-domain is called ARMA (auto regressive moving average) model. The EEG signals of *normal, epileptic* and *alcoholic* were analyzed using power spectra densities using fast Fourier transform (FFT) by Welch method, auto regressive (AR) Yule-Walker and Burg's method [21]. They have used first three peak power and peak frequencies of the power spectrum for the analysis.

Among the three parametric methods, AR method is widely used for the analysis. Burg's AR method is discussed below.

Burg method Burg method is based on minimizing forward and backward prediction errors while satisfying the Levinson-Durbin recursion [67, 56, 82]. In this method instead of calculating autocorrelation function, reflection coefficients are estimated directly. The primary advantages of this method are resolving closely spaced sinusoids in signals with low noise levels, and estimating short data records, in cases where the AR power spectral density estimates are very close to the true values. In addition, the Burg method ensures a stable AR model and is computationally efficient. The accuracy of this method is lower for high-order models, long data records, and high signal-to-noise ratios (which can cause line splitting, or the generation of extraneous peaks in the spectrum estimate). The spectral density estimate computed by the Burg method is also susceptible to frequency shifts (relative to the true frequency) resulting from the initial phase of noisy sinusoidal signals. This effect is magnified when analyzing short data sequences. Burg Method differs from Yule-Walker Method in the way the PSD, $P_{xx}^{BU}(f)$, is obtained, as shown in the following equation:

$$P_{xx}^{BU}(f) = \frac{\hat{e}_p}{\left|1 + \sum_{l=1}^{p} \hat{a}_p(l) e^{-2jfl}\right|^2} \tag{6}$$

where $\hat{e}_p$ denotes the total least square error and it is the sum of the forward and backward prediction errors.

$$\hat{e}_{f,p}(n) = x(n) + \sum_{i=1}^{p} \hat{a}_{p,i} x(n-i), \quad n = p+1, \ldots, U \tag{7}$$

$$\hat{e}_{b,p}(n) = x(n-p) + \sum_{i=1}^{p} \hat{a}^{*}_{p,i} x(n-p+i), \quad n = p+1, \ldots, U \tag{8}$$

For both, Burg and Yule Yule-Walker, the model order was chosen as the one that minimizes the Akaike information criterion (AIC) figure of merit [4, 5].

$$AIC(p) = N \cdot In\left(\hat{\lambda}^2\right) + 2p \tag{9}$$

where N is the number of data samples and $\hat{\lambda}^2$ is the estimated white noise variance. To reduce computational complexity, we assumed as optimal the value of p that fulfilled the AIC criterion in the first two epochs. One of the most important aspects of the AR method is the selection of the order p. For EEG signal modeling, the order of the model can be taken as: p=20 [21]. Figure 2 shows the frequency plot of EEG signal (Fig. 1) using FFT with Burg's method.

Short time fourier transform (STFT)

Fourier Transform is not suitable for analyzing non-stationary signals. A signal of finite length is expressed as the sum of frequency components of infinite duration. It fails to provide the exact location of an 'event' along the time scale in the frequency domain. In STFT, the signal is divided into small segments and the signal within this segment is assumed to be stationary. For this purpose, a window function, whose width is equal to the segment of the signal is chosen.

The definition of the STFT is:

$$STFT_x^{(w)}(t,f) = \int_{-\infty}^{\infty} [x(t).w^*(t-t')] .e^{-j2\pi ft} dt \qquad (10)$$

where,

$x(t)$ is the signal
$w(t)$ is the window function and * is the complex conjugate.

The drawback of STFT is the finite length window. The narrow window offers better time resolution and poor frequency resolution. And wider window results in good frequency resolution and poor time resolution. These wide windows may violate the condition of stationarity. Hence, the resolution is a problem in STFT and it can be resolved using wavelet transform [68].

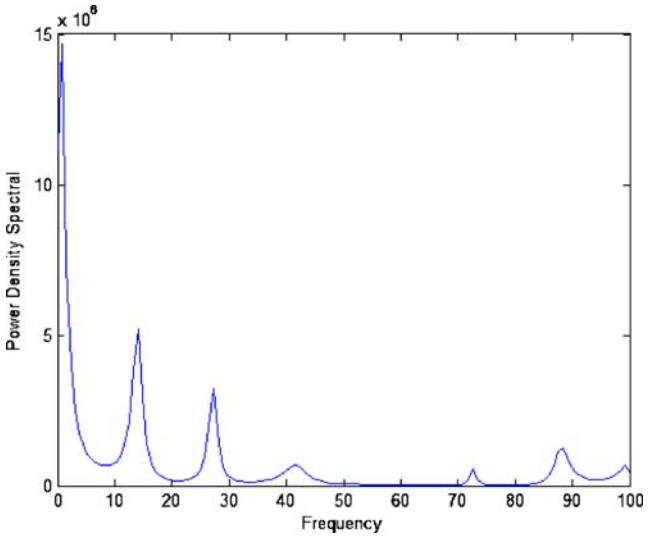

Fig. 2 Frequency plot of FFT with Burg's method for Fig. 1

Wavelet transform

Wavelet transform replaces the sinusoidal waves of Fourier transforms by translations and dilations of a window function called 'wavelet'. There are two types of wavelets transforms (i) discrete wavelet transform (DWT) (ii) continuous wavelet transform (CWT).

DWT provides sufficient information both for analysis and synthesis of the original signal, with a significant reduction in the computation time. The filters of different cutoff frequencies can be used to analyze the signal at different scales. The signal is passed through a series of high pass filters to analyze the high frequencies, and it is passed through a series of low pass filters to analyze the low frequencies. It is widely used for compression and noise reduction. Figure 3(a) shows the DWT coefficients using Daubechies 8 as mother wavelet for the EEG signal shown in Fig. 1. This method can be used to extract alpha, beta, theta and gamma frequencies of the EEG.

'*Wavelet*' is a wave of finite duration and finite energy, which is correlated with the signal to obtain the wavelet coefficients [89, 25]. The *mother wavelet* is a reference wavelet, whose coefficients are evaluated for the entire range of dilation and translation factors [25, 89]. The mother *wavelet* is shifted continually along the time scale for evaluating the set of coefficients at all instants of time. In the next phase, the wavelet is dilated for a different width and normalized to contain the same amount of energy as the mother wavelet. This process is repeated for the entire signal. Thus CWT is computed by changing the scale of the analysis window, shifting the window in time, multiplying by the signal, and integrating over all times. This process produces wavelet coefficients that are functions of scale and position. The wavelet coefficients are shown as pixel intensity (color), in a two dimensional plane with y-axis representing the dilation (scaling factor) of the wavelet, and the x-axis, its translation (time axis). Thus the wavelet transform plot (*scalogram*) is a 2D color pattern depicting the location of the 'event' occurring in the time scale.

The EEG signals were decomposed into frequency sub bands using discrete wavelet transform and later fed to the neural network for classification into epileptic or normal signal [35]. Figure 3(b) shows the CWT of the EEG signal shown in Fig. 1. These CWT coefficients can be used as features to identify the particular disease.

Nonlinear methods of analysis

Nonlinear techniques describe the signals generated by biological systems in a more effective way. Different nonlinear

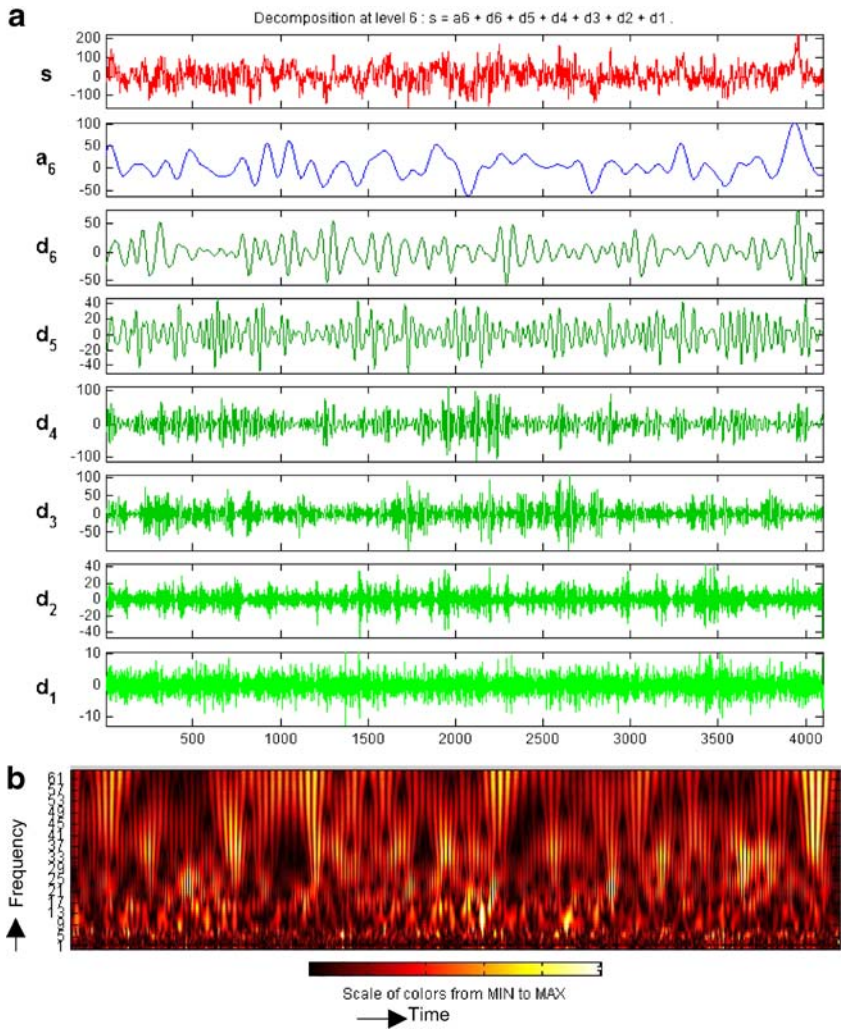

Fig. 3 **a** DWT of the EEG signal shown in Fig. 1. **b** CWT of the EEG signal shown in Fig. 1

parameters, like HOS, phase space plot, FD, CD, LLE, entropies, and recurrence plot are discussed in the following sections.

Higher order spectra

The HOS techniques find wide applications in the field of economics, speech, seismic data processing, plasma physics, and optics. They are also known as polyspectra, the spectral representations of higher order statistics, i.e. moments and cumulants of third order and beyond. The weak, high noise signals showed good results to the HOS. The study of HOS has been dominated by work on bispectrum.

Second order statistics form the basis of HOS analysis. Second order statistics deal with mean value m and variance σ^2. They are defined by expectation operation E [.], where "a" is the result of a random process.

$$m_a = E\{A\} \tag{11}$$

$$\sigma_A^2 = E\left\{(A - m_a)^2\right\} \tag{12}$$

If 'a' is the discrete time signal, the second order moment autocorrelation function (ACF) is defined as:

$$m_a^2(i) = E\{A(n).A(n+i)\} \tag{13}$$

In addition to these moments, HOS provides higher order moments, m^3,m^4,… and non linear combinations of the higher order moments, as cumulants $.c^1$,c^2,c^3…,. So, HOS consists of moment and cumulant spectra. Therefore it can be defined for both deterministic signals and random processes [58]. The EEG signal is therefore analyzed using different HOS that are spectral representations of higher order moments or cumulants of a signal. The Fourier Transform of the third order cumulant generating function is called the bispectrum given by

$$B(f_1,f_2) = E\left[X(f_1)X(f_2)X^*(f_1+f_2)X^*(f_1+f_2)\right] \tag{14}$$

where $X(f)$ is the Fourier transform of the signal $x(nT)$.

These fall in the category of higher order spectra and provide information in addition to the power spectrum. In practice, the expectation operation is replaced by an estimate that is an average over an ensemble of realizations of a random signal. For deterministic signals, the relationship holds without an expectation operation with the third order correlation being a time-average. For deterministic sampled signals, *X(f)* is the discrete-time Fourier transform and in practice it is computed as the discrete Fourier transform (DFT) at frequency samples using the FFT algorithm. The frequency *(f)* may be normalized by the Nyquist frequency to be between 0 and 1.

EEG signals monitoring has been mainly carried by Bispectrum measurements.

The bispectrum may be normalized (by power spectra at component frequencies) such that it has a value between 0 and 1, and indicates the degree of phase coupling between frequency components [58]. The normalized bispectrum or bicoherence is given by

$$B_{co}(f_1,f_2) = \frac{E(X(f_1)X(f_2)X^*(f_1+f_2)]}{\sqrt{P(f_1)P(f_2)P^*(f_1+f_2)}} \quad (15)$$

where *P(f)* is the power spectrum, f_1 and f_2 are normalized frequencies in the bispectrum.

Higher order spectral features Quantitative features are required to differentiate the distribution of bispectra from different EEG signals. Studies have shown that the signal shape is a function of its phase [60] and signals with different wave shapes may have the same power spectrum. The phases of the integrated bispectrum are used as a measure of the wave shape characteristics [11].

The bispectrum of a real signal is uniquely defined with the triangle $0 \le f_2 \le f_1 \le (f_1+f_2) \le 1$ by virtue of its symmetric properties, provided there is no bispectral aliasing. The bispectral values are integrated along straight lines with slope a passing through the origin in the bifrequency space, as shown in Fig. 4. The bispectral invariant, *P (a)*, is the phase of the integrated bispectrum along the radial line , given by,

$$P(a) = \arctan\left(\frac{I_i(a)}{I_r(a)}\right) \quad (16)$$

where

$$I(a) = I_r(a) + jI_i(a) \quad (17)$$

$$= \int_{f_1=0^+}^{\frac{1}{1+a}} B_{co}(f_1, af_1)df_1$$

for $0 < a \le 1$, and $j=\sqrt{-1}$. The variables I_r and I_i refer to the real and imaginary part of the integrated bispectrum respectively.

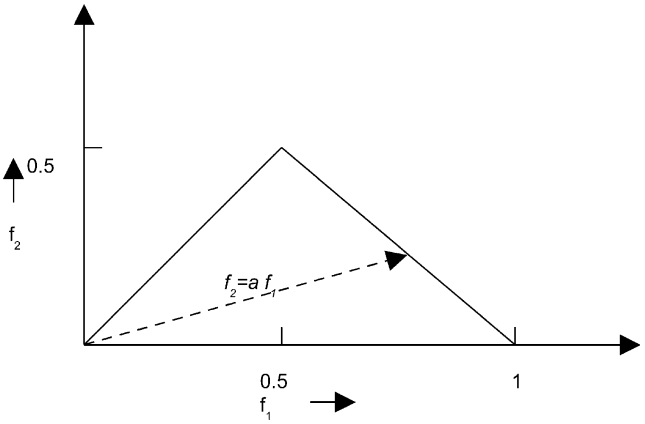

Fig. 4 Region of computation of the bispectrum for real signals. Features are calculated by integrating the bispectrum along the dashed line with slope = a. Frequencies are shown normalized by the Nyquist frequency

P(a), the bispectral invariants, contain information about the waveform shape within the window . Furthermore they are invariant to shift and amplification and robust to time-scale changes. However, they are particularly sensitive to changes in the left-right waveform asymmetry. For windowed segments of a white Gaussian random process, these features tend to be distributed symmetrically and uniformly about zero in the interval $[-\pi,+\pi]$. If the process is chaotic and exhibits a colored spectrum with third order time-correlations or phase coupling between Fourier components, mean value and distribution of the invariant feature may be used to identify the process. Sandha et al have analyzed the phase correlations in human EEG signal. It was found that there are high frequency components in the bicoherence of epileptic EEG signal which are otherwise absent. It was also noted that the bicoherence magnitude can be used to estimate the amount of phase coupling [74]. Figure 5 shows bispectrum and bicoherence plot of the EEG signal shown in Fig. 1. These plots are unique for normal EEG signals and peak amplitudes exist at (10, 10) Hz. These plots can be used to identify epileptic and preictal EEG signals [13].

State space reconstruction

State-space (also called phase-space) reconstruction is the first step in nonlinear time series analysis. It basically views a single-dimensional data series, $s(n);n=1,2,3,\ldots,N$, in an m-dimensional Euclidean space, R^m. Using this method, the trajectories that connect data points (vectors) in the state-space are expected to form an attractor that preserves the topological properties of the original unknown attractor. A common way to reconstruct the state-space is the method of delays introduced by Takens [85]. In this method, m-dimensional vectors, x_n in the state-space are formed from

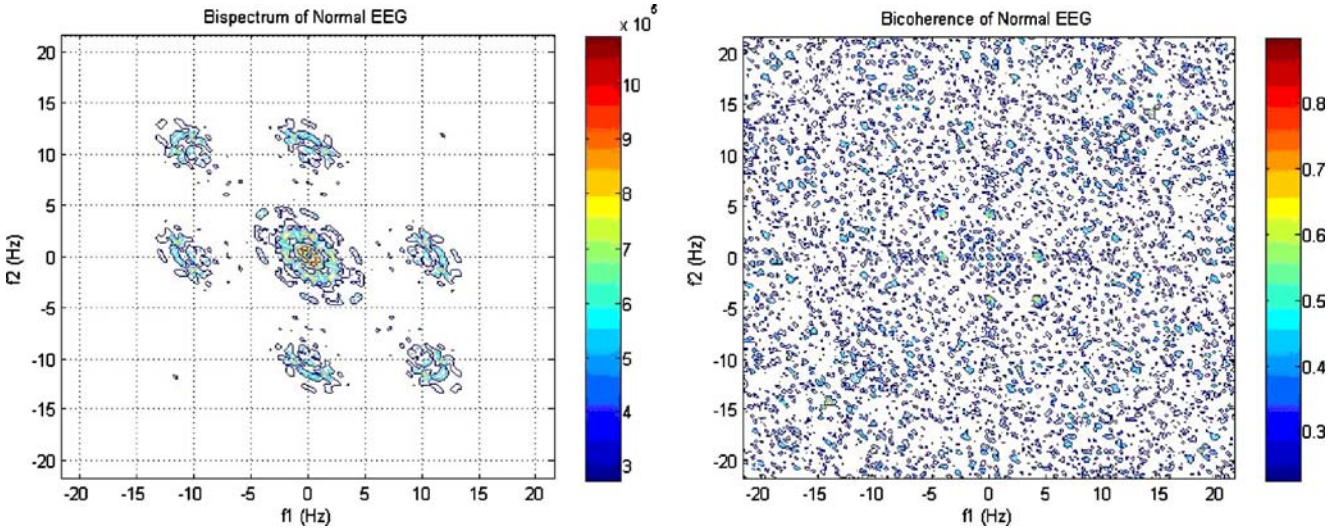

Fig. 5 Bispectrum and bicoherence plot of the signal shown in Fig. 1

the time-delayed samples of the original signal, *s(n)*, as follows:

$$x_n = [s(n),\, s(n-\lambda),\, s(n-2\lambda),\, \ldots\ldots,s(n-(m-1)\lambda] \qquad (18)$$

where λ is the embedding delay, and m is the embedding dimension (number of coordinates). The space constructed by using the vectors x_n is called the reconstructed space. Delay reconstruction requires a proper choice of the parameters λ and m. The value of λ can be calculated as the time (in samples) of the first zero crossing of the autocorrelation function. Sauer *et al* have generalized the Taken's theorem to find an optimal embedding dimension [75]. The number of false nearest neighbors becomes zero or drop off dramatically when the optimal embedding dimension, m is reached [54]. In practical applications, the Grassberger-Procaccia algorithm is used to measure the correlation dimension of reconstructions for different embedding dimensions [26].

Estimation of embedding dimension (m) False nearest neighbor (FNN) method can be used to determine the minimal sufficient embedding dimension (m) [45]. Let m_0 be the minimal embedding dimension for a given time series $\{S_i\}$. This means that in a m_0-dimensional delay space the reconstructed attractor is a one-to-one image of the attractor in the original phase space. Thus the neighbors of a given point will be mapped onto neighbors in the delay space. Due to the assumed smoothness of the dynamics, neighborhoods of the points are mapped onto neighborhoods again. The shape and the diameter of the neighborhoods is changed according to the Lyapunov exponents. The topological structure is not preserved due to the projections, if we choose, $m < m_0$. In the higher dimensions, points are projected into neighbourhoods of other points to which they do not belong. These points are the *false neighbors*.

For each point $\vec{S_i}$ in the time series, let $\vec{S_j}$ be the look for its nearest neighbor in m dimensional space. The distance between them is given by $\left\|\vec{s_i} - \vec{s_j}\right\|$. Iterate both points and compute

$$R_i = \frac{\left|s_{i+1} - s_{j+1}\right|}{\left\|\vec{s_i} - \vec{s_j}\right\|} \qquad (19)$$

R_t is the threshold point having false nearest neighbor. We should choose, embedding dimension high enough so that, fractional points for which $R_i > R_t$ is zero or very small.

In our case, we obtained the m as 10. Figure 6 shows the estimation of the embedding dimension for our data using FNN method.

Estimation of delay time (τ) Fraser *et al*, have suggested the time delayed mutual information to determine the reasonable time delay [24]. Unlike the autocorrelation function, this mutual information method takes into account the nonlinear correlations. It is given by:

$$S = -\sum_{ij} p_{ij}(\tau) In \frac{p_{ij}}{p_i p_j} \qquad (20)$$

Where, p_i is the probability to find a time series value in the i-th interval, and $p_{ij}(\tau)$ is the joint probability that an observation falls into the i-th interval and the observation time τ later falls into the j-th. As τ is increased, S decreases, and then rises again. The value of time delay where S

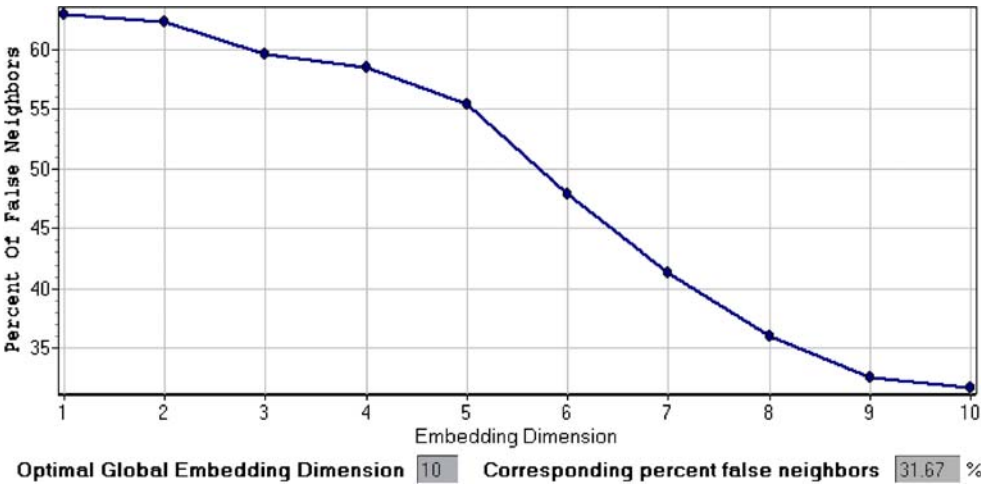

Fig. 6 Result of estimation of embedding dimension for the signal shown in Fig. 1

reaches its first minimum is the optimal τ for use in state space reconstruction [24].

Mutual information function for our EEG signal (Fig. 1) is given in Fig. 7. It can be clearly seen that the mutual information *S* reaches its first minimum at τ=8. Hence the optimal embedding delay (τ_{opt}) is determined using mutual information function in this study. We have obtained the time delay of 8 for the EEG signal (Fig. 1) used.

Phase space plot

The phase-space plot shown X-axis represents the *heart-rate* X[n] and the Y-axis represents the *heart-rate after a delay* X[n+τ] [78]. The time delay,τ is calculated using the minimal mutual information technique [23, 24]. Grassberger *et al*, have proposed a method of estimating the embedding dimension from the phase space patterns [27]. Ding.M *et al*, has verified that the embedding theorem restriction is sufficient, but not a necessary condition for dynamic reconstruction [18]. Nevertheless, the dimensionality of the attractor is usually unknown for experimental data and therefore, the corresponding embedding dimension is unknown. The embedding dimension is calculated from the delay-embedding theorem [85]. The accuracy of nonlinear time series analysis lies in the selection of an optimum embedding dimension [61]. Figure 8 shows the phase space plot of the normal EEG signal (shown in Fig. 1) [39]. The spread of the plot is different for different types of EEG signals [39]. The method to find the delay and embedding dimension are given in the following sections.

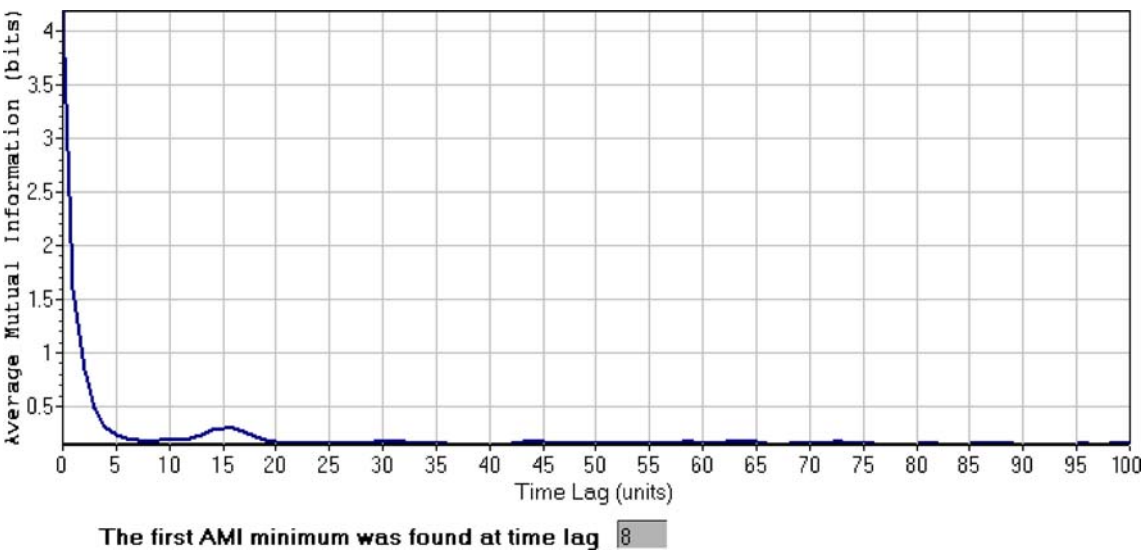

Fig. 7 Estimation of the delay using average mutual information

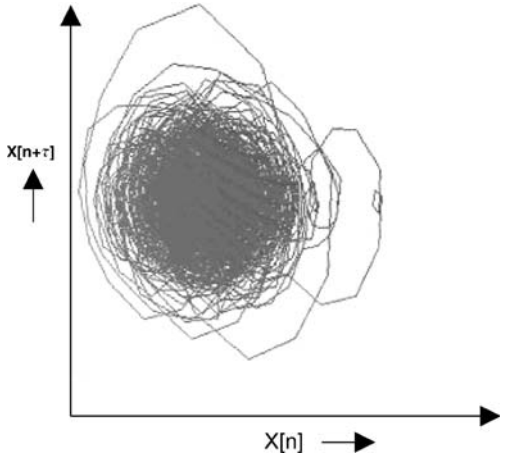

Fig. 8 Result of phase space plot for the signal shown in Fig. 1

Correlation dimension (CD)

Correlation dimension is one of the most widely used measures of fractal dimension. Grassberger *et al*, have proposed the method of estimating the embedding dimension from the phase space patterns [26]. A correlation integral function *C(r)* indicates the measure of the probability of two points on the trajectory that are separated by a distance r. A CD can be calculated using the distances between each pair of points in the set of N number of points, $s(x,y) = |X_x - X_y|$. CD is calculated as

$$CD = \lim_{r\to 0} \frac{\log C(r)}{\log(r)} \tag{21}$$

and Correlation integral *C(r)* is given by

$$C(r) = \frac{1}{N^2} \sum_{x=1}^{N} \sum_{y=1, x\neq y}^{N} \Theta\left(r - |X_x - X_y|\right) \tag{22}$$

where

X_x , X_y → points of the trajectory in the phase space
N → is the number of data points in phase space
r → radial distance around each reference point X_i
Θ→ is the Heaviside function.

The Correlation Dimension for the signal shown in Fig. 1 is 5.022. A decrease in CD indicates the brain dysfunctions in people suffering from Alzheimer's disease [17].

Fractional dimension (FD)

It is useful in quantifying the complexity of dynamic signals in biology and medicine. A fractal is a set of points which, when looked at smaller scales, resembles the whole set [55]. The FD of a waveform represents a powerful tool for transient detection. This feature has been used in ECG and EEG analysis to identify and distinguish specific states of physiologic functions [2].

Let S be a compact subset of a metric space. For each $\in > 0$, let $N(\in)$ be the smallest number of circles of radius $\leq \in$ necessary to cover S. Suppose

$$\delta = -\lim_{\in\to 0^+} \frac{\log N(\in)}{\log \in} \tag{23}$$

exists. Then δ is called the fractal dimension of S. It was shown that during the movement and holding periods, FDs of the EEG signals increased linearly with handgrip force [52]. FD has been used as a tool to characterize the complexity for short EEG time series [32]. The algorithms used to determine the FD of EEG signals are Katz algorithm and Higuchi's algorithm.

Higuchi's algorithm For the EEG sequence $x(1)$, $x(2)$,…, $x(N)$, s new sequence x_p^s is constructed as $x_p^k = \left\{x(p), x(p+s), x(p+2s), ..., x(p+\left[\frac{N-p}{s}\right]s), \right\}$ for p=1, 2, …, s, where p indicates the initial time value, and s indicates the discrete time interval between points. For each of the s series or curves x_p^k, the length $L_p(s)$ is computed by,

$$L_p(s) = \frac{\sum_{i=1}^{\lfloor a \rfloor} |x(p+is) - x(p+(i-1)s)|(N-1)}{\lfloor a \rfloor s} \tag{24}$$

where N is the total length of the data sequence x, (N–1)/$\lfloor a \rfloor s$ is a normalization factor and $a = \frac{N-p}{s}$, and $\lfloor a \rfloor$ means the integer part of a. An average length is computed as the mean of the s lengths $L_p(s)$ for p=1,2,….s. This procedure is repeated for each s ranging from 1 to s_{max} (in this work, $s_{max=128}$) obtaining an average length for each s. The graph of $\ln(L_p(s))$ versus $\ln(1/s)$ is plotted. The slope of the least-squares linear best fit gives the estimate of the fractal dimension ($D^{Higuchi}$)[31].

Katz algorithm FD for using Katz's method [43] for EEG signal is given by:

$$D^{Katz} = \frac{\log_{10}(L)}{\log_{10}(d)} \tag{25}$$

where L is the sum of distances between successive points, and d is the distance between the first point of the sequence and the point of the sequence that provides the farthest distance. Mathematically, d is expressed as $d = \max(\|x(1), x(i)\|); \quad i = 2, \ldots N.$

D^{Katz} compares the actual number of units that compose a curve with the minimum number of units required to reproduce a pattern of the same spatial extent. FD computed in this fashion depend on the measurement units used. This problem is solved by creating a general unit or yardstick: the average step or average distance between

successive points, δ. Normalizing the distances D^{Katz} is given by,

$$D^{Katz} = \frac{\log_{10}(L/\delta)}{\log_{10}(d/\delta)}. \quad (26)$$

The FD value using Higuchi's algorithm for the typical signal shown in Fig. 1 is 1.8650.

Largest lyapunov exponent (LLE)

The Lyapunov Exponent (λ) is used to discriminate between chaotic dynamics and periodic signals. It is a measure of the rate at which the trajectories separate from one another. Thus, λ provides a qualitative and quantitative characterization of dynamical behavior, and are related to the exponentially fast divergence or convergence of nearby orbits in phase space. Lyapunov exponents quantify the mean rate of divergence of neighbored trajectories along various directions in phase space. If a system has one or more positive Lyapunov exponents, then the future state of the system with an uncertain initial condition cannot be predicted. This type of system is known as chaotic. A positive Lyapunov exponent effectively represents a loss of system information [14]. For converging trajectories, the corresponding Lyapunov exponents are negative. A zero exponent means the orbits maintain their relative positions and they are on stable attractors. Finally, a positive exponent implies the orbits are on a chaotic attractor. The algorithm proposed by Wolf *et al* can be used to extract largest LLE from EEG data [92].

Let X_0 and $X_0 + \Delta x_0$ be the two EEG data points in a space. Let us assume that, each of them will generate an orbit in that space and the separation between the two orbits is Δx. This separation has the form $\Delta x(X_0,t)$ and will behave erratically. The mean exponential rate of divergence of two initially close orbits is given by

$$\lambda = \lim_{t\to\infty} \frac{1}{t} \ln \frac{|\Delta x(X_0,t)|}{|\Delta X_0|} \quad (27)$$

The maximum value of λ is called the largest Lyapunov exponent and is useful for distinguishing among the various types of orbits.

The time delay (τ) and the embedding dimension which are required for the calculation of LLE are evaluated using actual mutual information method and false nearest neighbor method respectively. According to Das et al [17] an embedding dimension between 5 and 20 as well as a delay of 1 should be chosen when calculating LE for EEG data. An embedding dimension of 10 and a delay of 1 was used for calculating LLE for the plot shown in Fig. 1. The value of LLE for the signal shown in Fig. 1 is 0.175.

Hurst exponent (H)

H can be used to evaluate the presence or absence of long range dependence and its degree in a time series. H is a measure of the smoothness of a fractal time series based on the asymptotic behavior of the rescaled range of the process. It was used for characterizing non stationary behavior present in sleep EEG episodes [15].The Hurst exponent is defined as

$$H = \frac{\log(R/S)}{\log(T)} \quad (28)$$

where

T is the duration of the sample of data
R/S is the corresponding value of rescaled range
R is the difference between the maximum deviation from the mean and minimum deviation from the mean
S is the standard deviation.

The values of the H vary between 0 and 1, with higher values indicating a smoother trend, less volatility, and less roughness. The Hurst exponent is 0.3527239 for the signal shown in Fig. 1.

Entropy estimators

Entropy measures the disorder in a signal. There are several analytical techniques used to quantify irregularities of time signals [59]. Entropy is proportional to the logarithm of the number of microstates available to a thermodynamic system, thus being related to the magnitude of system disorder. Shannon applied the concept of information or logical entropy to information theory and data communications. Recently, a number of different entropy estimators have been applied to quantify the complexity of signals [28]. Entropy estimators are broadly classified into two categories: a) spectral entropies and b) embedding entropies.

Spectral entropies The spectral entropies use the amplitudes of the power spectrum of the signal as the probabilities in entropy calculations. Shannon spectral entropy and Renyi's entropy are discussed in the following sections.

Spectral entropy Spectral entropy measures the irregularity or complexity in the EEG signals [34, 22].

S is given by:

$$S = \frac{\sum p_k \log p_k}{\log(N)} \quad (29)$$

where

P_k are spectral amplitudes of k frequencies region
N = number of frequencies.

The power spectral density (PSD) represents the distribution of power as function of frequency. The Shannon spectral entropy is −9.1586 for Fig. 1.

Renyi's Entropy (REN) Rényi entropy [70] is defined as:

$$H_m = \varphi^{-1}\left(\sum_f p_f \varphi(T(p_f))\right) \tag{30}$$

where $\varphi(.)$ is a continuous and strictly monotonic function subclass of Kolmogorov-Nagumo functions. To satisfy the constraints of an information measure,

$$\varphi(x) = \begin{cases} x & Shannon's\ entropy \\ 2^{(1-\alpha)x} & Renyi's\ entropy\ with\ order\ \alpha \end{cases}$$

Hartley's information measure is used as the information measure $T(pf) = -\log(pf)$. Simplifying the above relation *REN* is given by

$$REN = -\frac{1}{1-\alpha}\log\left(\sum_f p_f^{\alpha}\right); \quad \alpha > 0, \alpha \neq 1 \tag{31}$$

where $a \neq 1$.

The Renyi's entropy value for the typical signal shown in Fig. 1 is −0.1929.

Embedding entropies Embedding entropies use the time series directly to estimate the entropy. Kolmogorov-Sinai entropy and approximate entropy are discussed in this section

Kolmogorov sinai entropy (KS-entropy) It provides a quantitative measure for the degree of unpredictability within time-series signals. Entropy is determined from the embedded time series data by finding points on the trajectory close together in phase space but which occurred at different times (i.e., are not time correlated). These two points are then followed into the future to observe how rapidly they move apart from one another. The time it takes for point pairs to move apart is related to the so-called Kolmogorov entropy, which is denoted by K in the following equation.

$$\langle t_{div} \rangle = 2^{-Kt} \tag{32}$$

where $\langle t_{div} \rangle$ is the average time for the pair to diverge apart and K is expressed in bits per second [42].

The calculation of K from a time series typically starts from reconstructing the sytem's trajectory in an embedding space. According to Grassberger and Procaccaia [27], K can be determined from the correlation function $C_m(\mathrm{r}, \mathrm{N}_m)$ as

$$K = \lim_{r\to 0}\lim_{m\to\infty}\frac{1}{\tau}\frac{C_m(r, N_m)}{C_{m+1}(r, N_{m+1})} \tag{33}$$

where,

$$C_m(r, N_m) = \frac{2}{N_m(N_m-1)}\sum_{i=1}^{N_m}\sum_{\substack{j=1 \\ j\neq i}}^{N_m}\Theta\left(r - \left\|\mathbf{x}_i - \mathbf{x}_j\right\|\right) \tag{34}$$

where x_i and x_j are the points of the trajectory in the phase space, r is the radial distance around each reference point x_i, Θ is the Heaviside function and $N_m = N-(m-1)\tau$ is the number of points in the multidimensional state space. N represents the total number of data points, m represents the embedding dimension and τ represents the time lag. Entropy reflects how well one can predict the behavior of each respective part of the trajectory from the other. Higher entropy indicates less predictability and a closer approach to stochasticity. The K-S entropy value for the typical signal shown in Fig. 1 is 0.6034.

Approximate Entropy (ApEn) ApEn, quantifies the complexity and regularity of a system. A low ApEn value often indicates predictability and high regularity of time series data. High ApEn indicates unpredictability and random variation. It can be applied to relatively short and noisy data [63]. It detects the changes in underlying episodic behavior which are not reflected in peak occurrences or amplitudes [65]. ApEn assigns a nonnegative number to a time series, with larger values corresponding to more complexity or irregularity in the data. For N data points *x(1),x(2),…,x(N)*, with an embedding space of $\Re^m$, the ApEn measure is given by

$$ApEn(m, r, N) = \frac{1}{N-m+1}\sum_{i=1}^{N-m+1}\log C_i^m(r) - \frac{1}{N-m}\sum_{i=1}^{N-m}\log C_i^{m+1}(r) \tag{35}$$

where $C_i^m(r) = \frac{1}{N-m+1}\sum_{j=1}^{N-m+1}\left(r - \left\|x_i - x_j\right\|\right)$ is the correlation integral and N is the total number of data points. The values of m and r are chosen based on the results of previous studies by Pincus, indicating good statistical validity for ApEn [65]. The value of the ApEn for Fig. 1 is 2.1854.

Sample entropy (SampEn)

It is a refinement of the approximate entropy. *SampEn (m, r, N)* is the negative natural logarithm of the conditional probability that two sequences which are similar for m points remain similar at the next point. A lower value of SampEn indicates also a higher self-similarity in the time series. It is largely independent of record length and

displays relative consistency under circumstances where *ApEn* may not work well [71].

The *SampEn* can be defined as:

$$SampEn(m,r) = \lim_{N\to\infty}\left\{-\ln\left[C^{m+1}(r)/C^{m(r)}\right]\right\} \quad (36)$$

$C^m(r)$ is the probability that two sequence will match for m points and $C^{m+1}(r)$ is the probability that two sequence will match for m+1 points.

When the data length N is a limited value, the sample entropy estimated value can be expressed as:

$$SampEn(m,r,N) = -\ln\left[C^{m+1}(r)/C^{m}(r)\right] \quad (37)$$

where m is the length of sequence to be compared and r, the tolerance of accepting matches. N, m and r must be fixed for the calculation of SampEn. Different stages of sleep were analyzed using sample entropy and found that deeper sleep results in smaller SampEn values [36]. Bai et al, have found that SampEn is more sensitive to EEG changes caused by epilepsy than the *ApEn* method [6]. SampEn for Fig. 1 is 1.2309 .

Recurrence plot (RP)

RP reveals the nonstationarity of the time series. These plots disclose distance relationships between points on a dynamical system providing a faithful representation of time dependencies contained in the data [20]. It can be used for the diagnosis of drift and hidden periodicities in the signals. It also helps in visualizing the recurrence of states in phase space. Phase space does not have a dimension, but it allows us to visualize the high dimensional phase space by projecting it on to a lower dimensional sub-space. A recurrence of a state at time i and at a different time j is represented in a two-dimensional squared matrix (both axes being time axes) with ones and zeros shown by white and black dots in the plot. This representation is called recurrence plot. To obtain a recurrence plot from time series, the embedding dimension (m) is chosen by method of delays [1]. Figure 9 shows the recurrence plot of the original EEG signal shown in Fig. 1.

Surrogate data analysis

Surrogate data is the name for random data, generated to have the same mean, variance, and autocorrelation function as the original data. Surrogate data analysis techniques of time series signals can be used to test for nonlinear dynamics. The method of using surrogate in non linear time series analysis was introduced by Theiler *et al* [86]. It is obtained by phase randomizing the original data with spectral properties similar to the given data. In the case of data shuffling the histograms of the surrogate sequence and

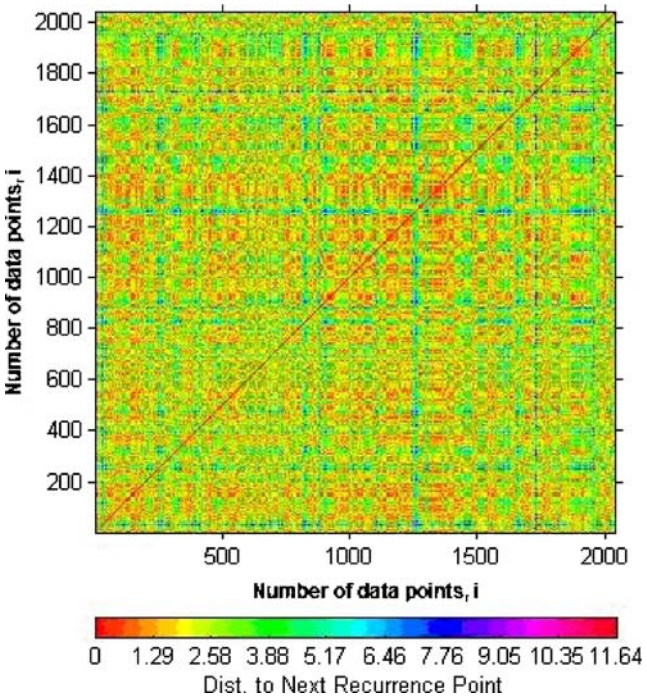

Fig. 9 Recurrence plot of the EEG signal shown in Fig. 1.(mark the axis

the reference sequence are identical [3]. The presence of non-linear dynamics is determined by comparing the non-linear parameter (say CD) calculated from original EEG data with the CD from phase-randomized surrogate data. If this CD in the two cases differ more than 50%, then the original signal is non-linear.

Discussion

EEG exhibits a significant non linear behavior [79]. Even though EEG signals are highly nonlinear, until recently linear methods were used for the analysis. Some of the linear methods used for analysis were Independent Component analysis (ICA), common spatial patterns (CSP), linear discrimination (LD) and linear prediction method. Researchers have studied time domain analysis of EEG signals [66, 87] and frequency domain methods for analysis [25, 35]. ICA separated the data into a set of temporally independent and spatially fixed components. The linear prediction (LP) method was used for analysis and presentation of spectral array data for the visualization of background EEG activity [66]. Statistical measures of variability are easy to compute and provide valuable prognostic information about patients. Time domain measures are susceptible to bias secondary to non-stationary signals. A potential confounding factor in characterizing variability with standard deviation is the increase in

baseline wander and artifacts. Another limitation of time domain measures is that they do not reliably distinguish between distinct biological signals. There can be many signals with identical means and standard deviations but with different underlying rhythms. Therefore, additional, more sophisticated methods of variability analysis are necessary to characterize and differentiate physiological signals. Hence, it is not encouraging to analyze the variability of signals using statistical measures to derive clinically useful information.

Analysis in the frequency domain was performed using Fourier or wavelet transform. Frequency domain analysis helps in characterising EEG signals as they fall in different frequency bands. Due to the limited frequency resolution of the STFT, wavelet transforms were found to be more suitable to EEG analysis. It is able to extract dynamical information from EEG signals. Kiymik *et al* have compared the performance of STFT and WT methods by evaluating epileptic seizure activity [44]. They observed that STFT method was good in processing real time signals due to its low computational complexity and wavelet methods can perform multiresolution analysis to eliminate noise at the same time [29]. Recently, Kiymik *et al* have presented time-frequency analysis of EEG signals during alert and drowsy state using DWT coefficients coupled with neural network [46]. In order to derive a valid and meaningful analysis using a FFT and frequency domain analysis, the assumptions of stationarity and periodicity are to be fulfilled. The signal must be periodic, having positive and negative alterations. In the interpretation of experimental data, periodic behavior may or may not exist when evaluating alterations in spectral power in response to intervention. The assumption of stationarity may also be violated when the signal is recorded for long durations. Spectral analysis is more sensitive to the presence of artifacts than time domain statistical methods.

Nonlinear dynamical analysis has been a powerful approach for understanding these physiological signals. It was observed that nonlinear dynamics theory would be a better approach than traditional time domain and frequency domain methods in analyzing and characterizing the EEG signals. HOS has been used as a tool for the analysis of non linear dynamic behavior of time series. This performs better when applied to weak and high noise signals. The HOS of Gaussian signals vanishes. Thus, it can be used to measure non-Gaussianity and to separate additive mixtures of independent non-Gaussian signals and Gaussian noise. This feature can be exploited to detect and classify non-Gaussian signals and provide high noise immunity in application where signal source is corrupted with Gaussian noise. The *normal*, *preictal* and *epileptic* EEG signals were successfully analyzed using HOS features [13]. The property of bispectrum preserves the phase information and is a useful tool for analyzing quadratic nonlinear interactions among different frequency components of a signal. Bicoherence was used to study the intracranial EEG signals during sleep, wakefulness and seizures [9]. Bullock *et al* have showed that maximum bispectrum, maximum power spectrum, maximum and mean bicoherence, skewness and asymmetry all vary independently during each sleep stage.

Carthy *et al*, have discussed different chaotic measures such as correlation dimension, Lyapunov exponent, Hurst exponent, fractal dimension and different entropies for the analysis of EEG [10].

The Lyapunov exponent is a measure for the rate at which nearby trajectories in phase space diverge. It has been used for the characterization of epileptic seizures [71, 84]. The minimum value of Lyapunov exponent indicates the seizure moment. The correlation dimension (CD) quantifies the nature of trajectory in a phase space plot [38]. A CD greater than 5 essentially implies a highly random data. The Hurst exponent characterizes the non-stationary behavior of EEG episodes. An exponent close to 0.5 implies that the signal is random and uncorrelated. It was observed that CD, LLE and Hurst exponent decreases during music and reflexological situations as the brain is devoid of any cognitive actions [39].

The ApEn have been used to measure the disorder in the EEG signals under conditions of anesthesia and determine the information flow in the brain [8, 81]. Fractal analysis can be used to investigate the relevant EEG events in a short data length by means of non-linear methods [32, 43].

These linear, time-frequency and non-linear techniques can be used to predict and analyze the mental diseases like epilepsy, autism, dementia, sleep apnea, effect of music and reflexological stimulation using EEG signals. The non-linear methods are very effective for the non-stationary, chaotic physiological signals. Hence, now a days, these techniques are increasingly used to unearth the hidden information from the EEG signals. The efficacy of different drugs on the different brain related diseases can be analyzed using these methods effectively. FPGA (field-programmable gate arrays) processors can be used to analyze the 24 h real time EEG data.

Conclusion

EEG signals can be used as an authentic indicator, which allows us to observe mental states and diseases related to the brain. The EEG signal is highly subjective and can be considered as a chaotic signal. The effect of various physiological events on the EEG signal has been discussed. Different signal analysis methods linear, frequency domain, time-frequency, and nonlinear techniques are also discussed. The linear and frequency methods are not very

effective in the analysis of the physiological signals. Hence the dynamical analysis methods can be applied to the complex series to investigate the behavior of biological systems. Nonlinear parameters have been used for the analysis of pathological signals and are good indicators of pathologies. The phenomenon that could not be detected by visual inspection of the EEG signal or by traditional methods of signal processing are effectively analyzed using nonlinear methods. The application of non-linear dynamical methods to the EEG signals has helped in understanding complex physiological phenomena such as abrupt transitions and chaotic behavior. Hence, the application of non-linear parameters to particular disease will be very useful for the clinicians. We have discussed different linear and non-linear techniques in this paper. The non-linear parameters such as correlation dimension, Hurst exponent (H), bispectrum features of the higher order spectra (HOS), largest Lyapunov exponents (LLE), different entropies, phase space and recurrence plots can be used for their analysis.

References

1. Abarbanel, H. D. I., *Analysis of observed Chaotic data*. Springer-Verlag:New York, 1996.
2. Acharya, U. R., Faust, O., Kannathal, N., Chua, T. J., and Laxminarayan, S., Dynamical analysis of EEG signals at various sleep stages. *Comput. Methods Programs Biomed*. 80(1):37–45, 2005 doi:10.1016/j.cmpb.2005.06.011.
3. Acharya, U. R., Joseph, P. K., Kannathal, N., Min, L. C., and Suri, J. S., Heart rate Variability: a review. *Med. Biol. Eng. Comput*. 44(12):1031–1051, 2006 doi:10.1007/s11517-006-0119-0.
4. Akaike, H., Fitting autoregressive models for prediction. *Ann. Inst. Stat. Math*. 21:243–247, 1969 doi:10.1007/BF02532251.
5. Akaike, H., A new look at statistical model identification. *IEEE Trans. Automat. Contr*. 19:716–723, 1974 doi:10.1109/TAC.1974.1100705.
6. Bai, D., and Li Qiu, T., The sample entropy and its application in EEG based epilepsy detection. *J. Biomed. Eng*. 24(1):200–205, 2007.
7. Bhattacharya, J., and Petsche, H., Phase synchrony analysis of EEG during music perception reveals changes in functional connectivity due to musical expertise.. *Signal processing*. 85 (11):2161–2177, 2005 doi:10.1016/j.sigpro.2005.07.007.
8. Bruhn, J., and Ropcke, H., Approximate entropy as an electroencephalographic measure of anesthetic drug effect during desflurane anesthesia.. *Anesthesilogy*. 92(3):715–726, 2000 doi:10.1097/00000542-200003000-00016.
9. Bullock, T. H., Achimowicz, J. Z., Duckrow, R. B., Spencer, S. S., and Iragui-Madoz, V. J., Bicoherence of intracranial EEG in sleep, wakefulness and seizures. *Electroencephalogr. Clin. Neurophysiol*. 103:661–678, 1997 doi:10.1016/S0013-4694(97)00087-4.
10. Carthy, RAMc., and Warrington, E. K., *Cognitive Neuropsychology: A clinical Introduction*. Academic Press:San Diego, LA, 1990.
11. Chandran, V., and Elgar, S., Pattern recognition using invariants defined from higher order spectra- one dimensional inputs. *IEEE Trans. Signal Process*. 41(1):205–212, 1993 doi:10.1109/TSP.1993.193139.
12. Charles, W. A., James, N. K., O'Connor, T., Michael, J. K., and Artem, S., Geometric subspace methods and time-delay embedding for EEG artifact removal and classification. *IEEE Trans. Neural Syst. Rehabil. Eng*. 14(2):142–146, 2006 doi:10.1109/TNSRE.2006.875527.
13. Chua, K. C., Chandran, V., Acharya, U. R., and Lim, C. M., Analysis of epileptic EEG signals using higher order spectra. *J. Med. Eng. Technol.* (2007) (in press).
14. Claesen, S., and Kitney, R. I., Estimation of the Largest Lyapunov Exponent of an RR Interval and its use as an Indicator of Decreased Autonomic Heart Rate Control. *Comput. Cardiol.* ▪▪▪, 133–136, (1994).
15. Dangel, S., Meier, P.F., Moser, H.R., Plibersek, S., and Shen, Y., Time series analysis of sleep EEG. *Computer assisted. Physics* ▪▪▪, 93–95, 1999.
16. Das, A., Das, P., and Roy, A.B., Applicability of Lyapunov Exponent in EEG data analysis. *Complexity International*. 2002.
17. Dias-Tosta, E., Kuckeihaus, G. S., Amaral, K., Sinha, J., Kurup, A., Paleti, A., et al., Decrease of non-linear structure in the EEG of Alzheimer patients compared to healthy controls. *Clin. Neurophysiol.* 110(7):1159–1167, 1999 doi:10.1016/S1388-2457(99)00013-9.
18. Ding, M., Grebogi, E., Ott, E., Sauer, T., and Yorke, J. A., Estimating correlation dimension from a chaotic time series:when a plateau occurs? *Physica. D.* 69:404–424, 1993 doi:10.1016/0167-2789(93)90103-8.
19. Durka, P. J., Klekowicz, H., Blinowska, K. J., Szelenberger, W., and Niemcewicz, S. Z., Simple system for detection of EEG artifacts in polysomnographic recordings. *IEEE Trans. Biomed. Eng.* 50(4):526–528, 2003 doi:10.1109/TBME.2003.809476.
20. Eckmann, J. P., Kamphorst, S. O., and Ruelle, D., Recurrence Plots of Dynamical Systems. *Europhys. Lett.* 4:973–977, 1987 doi:10.1209/0295-5075/4/9/004.
21. Faust, O., Acharya, U. R., Alen, A., and Lim, C. M., Analysis of EEG signals during epileptic and alcoholic states using AR modeling techniques. *Innovations and Technology in Biology and Medicine (ITBM-RBM).* 29(1):44–52, 2008.
22. Fell, J., and Roschke, J., A Comparison between spectral and nonlinear EEG measures. *Electroencephalogr. Clin. Neurophysiol.* 98(5):401–410, 1996 doi:10.1016/0013-4694(96)95636-9.
23. Fraser, A. M., Information and entropy in strange attractors. *IEEE Trans. Inf. Theory.* 35:245–262, 1989 doi:10.1109/18.32121.
24. Fraser, A. M., and Swinney, H. L., Independent coordinates for strange attractors from mutual information. *Phys. Rev. A* 33:1134–1140, 1986 doi:10.1103/PhysRevA.33.1134.
25. Gigola, S., Ortiz, F., D'Attellis, C. E., Silva, W., and Kochen, S., Prediction of epileptic seizures using accumulated energy in a multiresolution framework. *J. Neurosci. Methods.* 138(1–2):107–111, 2004 doi:10.1016/j.jneumeth.2004.03.016.
26. Grassberger, P., and Procassia, I., Measuring the strangeness of strange attractors. *Physica D* 9:189–208, 1983 doi:10.1016/0167-2789(83)90298-1.
27. Grassberger, P., and Procaccia, I., Characterization of strange attractors. *Phys. Rev. Lett.* 50(5):346–349, 1983 doi:10.1103/PhysRevLett.50.346.
28. Grassberger, P., and Schrieber, T., Nonlinear time sequence analysis. *Int. J. Bifurcat. Chaos.* 1(3):512–547, 1991 doi:10.1142/S0218127491000403.
29. Haselsteiner, E., and Pfurtscheller, G., Using time-dependent neural networks for EEG classification. *IEEE Trans. Rehabil. Eng.* 8:457–463, 2000 doi:10.1109/86.895948.
30. Hebert, R., Lehmann, D., Tan, G., Travis, F., and Arenander, A., Enhanced EEG alpha time-domain phase synchrony during

Transcendental Meditation: Implications for cortical integration theory. *J. Signal Process.* 85(11):2213–2232, 2005 doi:10.1016/j.sigpro.2005.07.009.
31. Higuchi, T., Approach to an irregular time series on the basis of the fractal theory. *Physica. D* 31:277–283, 1988 doi:10.1016/0167-2789(88)90081-4.
32. Hubert, P., Lutzenberger, W., Pulvermüller, F., and Birbaumer, N., Fractal dimensions of short EEG time series in humans. *Neurosci. Lett.* 225(2):77–80, 1997 doi:10.1016/S0304-3940(97)00192-4.
33. Hudson, D. L., Cohen, M. E., Kramer, M., Szeri, A., and Chang, F. L., *Diagnostic Implications of EEG Analysis in Patients with Dementia. Proceedings of 2nd International IEEE EMBS Conference on Neural Engineering*. 629–632, 2005
34. Inoye, K., Quantification of EEG irregularity by use of the entropy of the power spectrum. *Electroencephalogr. Clin. Neurophysiol.* 79:204–210, 1991 doi:10.1016/0013-4694(91)90138-T.
35. Jahankhani, P., Kodogiannis, V., and Revett, K., *EEG Signal Classification Using Wavelet Feature Extraction and Neural Networks. IEEE International Symposium on Modern Computing John Vincent Atanasoff*. 120–124, 2006
36. Jiayi, G., Peng, Z., Xin, Z., and Mingshi, W., Sample Entropy Analysis of Sleep EEG under Different Stages. IEEE/ICME Int. Conference on Complex Medical Engineering. 1499–1502, 2007
37. Joseph, P., Kannathal, N., and Acharya, U. R., Complex Encephalogram Dynamics during Meditation. *Journal of Chinese clinical medicine.* 2(4):220–230, 2007.
38. Kang-ming, C., and Pei-chen, L., Meditation EEG interpretation based on novel fuzzy-merging strategies and wavelet features. *Biomedical Engineering Applications. Basis Commun.* 17(4):167–175, 2005.
39. Kannathal, N., Acharya, U. R., Fadilah, A., Tibelong, T., and Sadasivan, P. K., Nonlinear analysis of EEG signals at different mental states. *Biomed. Online J.* 3:7, 2004 doi:10.1186/1475-925X-3-7.
40. Kannathal, N., Acharya, U. R., Joseph, P., and Ng, E. Y. K. Analysis of EEG signals with and without reflexology using FFT and auto regressive modeling techniques. *J. Chin. Clin. Med.* 1 (1):12–20, 2006.
41. Kannathal, N., Choo, M., Acharya, U. R., and Sadasivan, P., Entropies for detection of epilepsy in EEG. *Comput. Methods Programs Biomed.* 80(3):187–194, 2005 doi:10.1016/j.cmpb.2005.06.012.
42. Kantz, H., and Schreiber, T., *Nonlinear lime series analysis.* Cambridge University Press:New York. 1997
43. Katz, M., Fractals and the analysis of waveforms. *Comput. Biol. Med.* 18(3):145–156, 1988 doi:10.1016/0010-4825(88)90041-8.
44. Kemal, M. K., Guler, I., Alper, D., and Mehmet, A., Comparison of STFT and Wavelet Transform methods in determining epileptic seizure activity in EEG signals for real time application. *Comput. Biol. Med.* 35:603–616, 2005 doi:10.1016/j.compbiomed.2004.05.001.
45. Kennel, M. B., Brown, R., and Abarbanel, H. D. I., etermining embedding dimension for phase-space reconstruction using a geometrical construction. *Phys. Rev. A* 45:3403, 1992 doi:10.1103/PhysRevA.45.3403.
46. Kiymik, M. K., Akin, M., and Subasi, A., Automatic recognition of alertness level by using wavelet transform and artificial neural network. *J. Neurosci. Methods.* 139(2):231–240, 2004 doi:10.1016/j.jneumeth.2004.04.027.
47. Kobayashi, T., Misaki, K., Nakagawa, H., Madokoro, S., Ihara, H., Tsuda, K., et al., Non-linear analysis of the sleep EEG. *Psychiatry Clin. Neurosci.* 53(2):159–161, 1999 doi:10.1046/j.1440-1819.1999.00540.x.
48. Ktonas, P.Y., Golemati, S., Tsekou, H., Paparrigopoulos, T., Soldatos, C.,R., Xanthopoulos, P., et al., Potential dementia biomarkers based on the time-varying microstructure of sleep EEG spindles. *29th Annual International Conference of the IEEE Engineering in Medicine and Biology Society*. 2464–2467, 2007.
49. Lee, J., Kim, D., Kim, I., Suk Park, K., and Kim, S., onlinear-analysis of human sleep EEG using detrended fluctuation analysis. *Med. Eng. Phys.* 26(9):773–776, 2004 doi:10.1016/j.medengphy.2004.07.002.
50. Li, X., Sleigh, J. W., Voss, L. J., and Ouyang, G., Measure of the electroencephalographic effects of sevoflurane using recurrence dynamics. *Neurosci. Lett.* 424(1):47–50, 2007 doi:10.1016/j.neulet.2007.07.041.
51. Lin, R., Ren-Guey, L., Chwan-Lu, T., Heng-Kuan, Z., Chih-Feng, C., and Joe-Air, J. A., New Approach For Identifying Sleep Apnea Syndrome Using Wavelet Transform and Neural Networks. *Biomedical Engineering Applications-Basis & Communications.* 18 (3):138–144, 2006.
52. Liu, J. Z., Yang, Q., Yao, B., Brown, R. W., and Yue, G. H., Linear correlation between fractal dimension of EEG signal and handgrip force. *Biol. Cybern.* 93(2):131–140, 2005 doi:10.1007/s00422-005-0561-3.
53. Lu, H., Wang, M., and Yu, H., *EEG Model and Location in Brain when Enjoying Music*Proceedings of the 27th Annual IEEE Engineering in Medicine and Biology Conference Shanghai: China. 2695–2698, 2005.
54. Mahgoub, Y. A., and Dansereau, R. M.,Voicing-state classification of co-channel speech using nonlinear state-space reconstruction. *Proceedings of IEEE International Conference on Acoustics, Speech, and Signal Processing*. 409–412, 2005.
55. Mandelbrot, B. B., *Geometry of nature*. Freeman:Sanfrancisco, 1983
56. Marple, S. L., Digital Spectral Analysis. *Englewood Cliffs NJ, Prentice-Hall*, 1987, Chapter 7.
57. Martin, B., Milos, M., Ake, E., Katerina, C., and Vladimir, K., Objective assessment of the degree of dementia by means of EEG. *Neuropsychobiology.* 48:19–26, 2003 doi:10.1159/000071824.
58. Nikias, C. L., and Raghuveer, M. R., Bispectrum Estimation:A Digital Signal Processing Framework. *Proc. IEEE.* 75(7):869–891, 1987 doi:10.1109/PROC.1987.13824.
59. Nunes, R. R., de Almeida, M. P., and Sleigh, J. W., Spectral entropy: a new method for anesthetic adequacy. *Rev. Bras. Anestesiol.* 54(3):403–422, 2004.
60. Oppenheim, A. V., and Lim, J. S., The importance of phase in signals. *Proc. IEEE*. 69:529–550, 1981 doi:10.1109/PROC.1981.12022.
61. Packard, N. H., Crutchfield, J. P., Farmer, J. D., and Shaw, R. S., Geometry from a time series. *Phys. Rev. Lett.* 45:712–716, 1980 doi:10.1103/PhysRevLett.45.712.
62. Patil, S. T., and Bormane, D. S., Electroencephalograph Signal Analysis During Bramari. *9th Int. Conference on Inf.Technology (ICIT 06)*. 26–32, 2006.
63. Pincus, S. M., Approximate entropy as a measure of system complexity. *Proc. Natl. Acad. Sci. USA.* 88:2297–2301, 1991 doi:10.1073/pnas.88.6.2297.
64. Pincus, S. M., and Goldberger, A. L., Physiological time-series analysis: what does regularity quantify? Am. *J. Physiol.* 266: H1643–H1656, 1994.
65. Pincus, S. M., and Keefe, D. L., Quantification of hormone pulsatility via an approximate entropy algorithm. *Am. J. Physiol.* 262:E741–E754, 1992.
66. Pradhan, N., and Dutt, D. N., Data compression by linear prediction for storage and transmission of EEG signals. *Int. J. Biomed. Comput.* 35(3):207–217, 1994 doi:10.1016/0020-7101(94)90076-0.
67. Proakis, J., and Manolakis, D.,*Digital Signal Processing*. Prentice-Hall. 1996, Chapter 12.
68. Rao, R. M., and Bopardikar, A.S.,Wavelet Transforms introduction to theory and applications. *Addison Wesley, Longman Inc, Reading, MA*, 1998.

69. Renna, M., Handy, J., and Shah, A., Low Baseline Bispectral Index of the Electroencephalogram in Patients with Dementia. *Anesth. Analg.* 96:1380–1385, 2003 doi:10.1213/01.ANE.0000059223.78879.0F.
70. Renyi, A., On measures of entropy and information. *Proc. Fourth. Berkeley Symp. Math. Stat. Prob.* 1:547–561, 1961.
71. Richmann, J. S., and Moorman, J. R., hysiological time series analysis using approximate entropy and sample entropy. *Am. J. Physiol. Heart Circ. Physiol.* 278:2039–2049, 2000.
72. Robert, L., Ren-Gue, L., Chwan-Lu, T., heng-Kuan, Z., Chih-Feng, C., and Joe-Air, J., A new approach for identifying sleep apnea syndrome using wavelet transform and neural networks. Biomedical engineering-Applications. *Basis Commun.* 18:138–143, 2006.
73. Roháľová, M., Sykacek, P., Koskaand, M., and Dorffner, G., Detection of the EEG Artifacts by the Means of the (Extended) Kalman Filter. *Meas. Sci. Rev.* 1(1):59–62, 2001.
74. Sandha, G. S., Singh, P. K., Oberoi, N. D., and Nagchoudhuri, D., Phase Correlations in Human EEG Signal: A Case Study. *Second IEEE International Workshop on Electronic Design, Test and Applications.* 41 – 43, 2004.
75. Sauer, T., Yorke, J. A., and Casdagli, M., Embedology. *J. Stat. Phys.* 65:579–616, 1991 doi:10.1007/BF01053745.
76. Sheikhani, A., Behnam, H., Mohammadi, M. R., and Noorozian, M., Analysis of EEG background activity in Autism disease patients with bispectrum and STFT measure. *Proceedings of the 11th Conference on 11th WSEAS International Conference on Communications.* 11:318–322, 2007.
77. In-Ho, S., Doo-Soo, L., and Sun I, K., Recurrence quantification analysis of sleep electroencephalogram in sleep apnea syndrome in humans. *Neurosci. Lett.* 366(2):148–153 doi:10.1016/j.neulet.2004.05.025.
78. Srinivasan, N., Wong, M. T., & Krishnan, S. M. (2003). *A new Phase Space Analysis Algorithm for Cardiac Arrhythmia Detection* pp. 82–85. Mexico: Proceedings of the 25th Annual International Conference of the IEEE EMBS Cancun.
79. Stam, C. J., Pijn, J. P., Suffczynski, P., and da silva, F. H. L., Dynamics of the human alpha rhythm:evidence for online. *Clin. Neurophysiol.* 110:1801–1813, 1999 doi:10.1016/S1388-2457(99)00099-1.
80. Stanski, D. R., Using Pharmacodynamic Modelling of the Electroencephalogram (EEG) to understand anesthetic drug clinical pharmacology. *Drug Metab. Pharmacokinet.* 5(4):504–508, 1990.
81. Steyn-Ross, M. L., Steyn Ross, D. A., Sleigh, J. W., and Liley, D. T., Theoretical Electroencephalogram stationary spectrum for a white noise driven cortex:evidence for a general anesthetic-induced phase transition. *Phys. Rev. E Stat. Phys. Plasmas Fluids Relat. Interdiscip. Topics.* 60(6):7299–7311, 1999 doi:10.1103/PhysRevE.60.7299.
82. Stoica, .P, and Moses, R. L., *Introduction to Spectral Analysis*. Prentice-Hall, 1997.
83. Subasi, A., EEG signal classification using wavelet feature extraction and a mixture of expert model. *Expert Syst. Appl. An Int. J.* 32(4):1084–1093, 2007 doi:10.1016/j.eswa.2006.02.005.
84. Swiderski, B., Osowski, S., and Rysz, A., Lyapunov Exponent of EEG Signal for Epileptic Seizure Characterization. *Proceedings of the 2005 European Conference on Circuit Theory and Design.* 2 (28):153–156, 2005.
85. Takens, F., Detecting Strange Attractors in Turbulence. In D. Rand, L. S. Young (Eds.), *Dynamical Systems and Turbulence*. Springer: Berlin, 1981.
86. Theiler, J., Eubank, S., Longtin, A., Galdrikian, B., and Farmer, J. D., Testing for nonlinearity in time series: the method of surrogate data. *Physica D.* 58:77–94, 1992 doi:10.1016/0167-2789(92)90102-S.
87. Tzyy-Ping, J., Makeig, S., Mckeown, M. J., Bell, A. J., Te-Won, L., and Sejnowski, T. J., Imaging Brain Dynamics Using Independent Component Analysis. *Proc. IEEE.* 89(7):1107–1122, 2001 doi:10.1109/5.939827.
88. Venkatramanan, S., and Kalpakam, N. V., Aiding the detection of Alzheimer's disease in clinical electroencephalogram recording by selective de-noising of ocular artifacts. *International Conference on Communications, circuits and systems.* 2:965–968, 2004.
89. Vetterli, M., Wavelet anf filter banks:theory and design. *IEEE Trans. Signal Process.* 40(9):2207–2232, 1992 doi:10.1109/78.157221.
90. Wei-Chih, L., Hung-Wen, C., and Chien-Yeh, H., *Discovering EEG Signals Response to Musical Signal Stimuli by Time-frequency analysis and Independent Component Analysis*. Proceedings of the 27th Annual IEEE Engineering in Medicine and Biology Conference Shanghai:China. 2765–2768, 2005
91. Welch, P. D., The use of Fast Fourier Transform for the Estimation of Power Spectra: A Method based on time averaging over short, modified periodograms. *IEEE Trans Audio Electroacoust.* AU-15:70–73, 1967 doi:10.1109/TAU.1967.1161901.
92. Wolf, A., Swift, J. B., Swinney, H. L., and Vastano, J. A., Determining Lyapunov exponents from a time series. *Physica. D* 16:285–317, 1985 doi:10.1016/0167-2789(85)90011-9.